

[< Previous Article](#)

[Articles in Press](#)

[Next Article >](#)

Access this article on
[ScienceDirect](#)

Article in Press

Comprehensive use of cardiac computed tomography to guide left ventricular lead placement in cardiac resynchronization therapy.

[Jonathan M. Behar](#), MBBS, [Ronak Rajani](#), MD, [Amir Pourmorteza](#), PhD, [Rebecca Preston](#), MBBS, [Orod Razeghi](#), PhD, [Steve Niederer](#), PhD, [Shaunik Adhya](#), MD, [Simon Claridge](#), MBBS, [Tom Jackson](#), MBBS, [Ben Sieniewicz](#), MBBS, [Justin Gould](#), BSc, [Gerry Carr-White](#), PhD, [Reza Razavi](#), MD, [Elliot McVeigh](#), PhD, [Christopher Aldo Rinaldi](#), MD FHRS

[Open Access](#) | 0

DOI: <http://dx.doi.org/10.1016/j.hrthm.2017.04.041>

Open access funded by Wellcome Trust

[Article Info](#)

Article Tools

- [PDF \(1 MB\)](#)
- [Download Images\(.ppt\)](#)
[About Images & Usage](#)
- [Email Article](#)
- [Add to My Reading List](#)
- [Export Citation](#)
- [Create Citation Alert](#)
- [Cited by in Scopus \(0\)](#)

Related Articles

[Abstract](#) **[Full Text](#)** [Images](#) [References](#) [Supplemental Materials](#)

Article Outline

- I. [Introduction](#)
 - A. [Methods](#)
 1. [Pre assessment](#)
 2. [Cardiac CT](#)
 - B. [CRT implantation](#)
 - C. [Statistics](#)
- II. [Results](#)
 - A. [Quality of CT datasets](#)
 - B. [CT-SQUEEZ derived target segments to predict the optimal venous target](#)
 - C. [CT versus hemodynamic/electrical guidance \(figure 4\)](#)
 - D. [CRT response \(Table 2\)](#)
- III. [Discussion](#)
 - A. [The principal findings were:](#)
 - B. [Limitations](#)
- IV. [Conclusions](#)
- V. [Acknowledgement of support.](#)
- VI. [Appendix A. Supplementary data](#)
- VII. [References](#)

Abstract

Background

Optimal lead positioning is an important determinant of cardiac resynchronization therapy (CRT) response.

Objective

Evaluation of cardiac computed tomography (CT) selection of the optimal epicardial vein for LV lead placement by targeting regions of late mechanical activation (LMA) and avoiding myocardial scar.

Methods

18 patients undergoing CRT upgrade with existing pacing systems, underwent pre-implant ECG-gated cardiac CT to assess wall thickness, hypoperfusion, LMA and regions of myocardial scar by the derivation of the Stretch Quantifier of Endocardial Engraved Zones (SQUEEZ) algorithm. Cardiac venous anatomy was mapped to individualized AHA bulls-eye plots to identify the optimal venous target and compared with acute hemodynamic response (AHR) in each coronary venous target using an LV pressure wire.

Results

15 datasets were evaluable. CT-SQUEEZ derived targets produced a similar mean AHR compared with the best achievable AHR ($20.4 \pm 13.7\%$ vs. $24.9 \pm 11.1\%$, $p=0.36$). SQUEEZ derived guidance produced a positive AHR in 92% of target segments and pacing in a CT-SQUEEZ target vein produced a greater clinical response rate versus non-target segments (90 vs 60%).

Conclusion

Pre-procedural CT-SQUEEZ derived target selection may be a valuable tool to predict the optimal venous site for LV lead placement in patients undergoing CRT upgrade.

Key words:

[Cardiac computed tomography](#), [Cardiac resynchronization therapy](#), [Image guided intervention](#), [Dyssynchrony](#), [Myocardial fibrosis](#)

Introduction

Jump to Section

Go

Patients with existing pacing systems, LV systolic impairment and a high proportion of right ventricular (RV) pacing benefit from cardiac resynchronization therapy (CRT)¹. CRT non-response occurs due to suboptimal LV lead positioning in myocardial scar with persistent dyssynchrony^{2, 3}. Cardiac magnetic resonance (CMR) can guide LV lead placement avoiding scar and targeting late mechanical activation (LMA)⁴ however 28% patients undergoing CRT have existing pacing systems unsuitable for CMR⁵. Cardiac computed tomography (CT) has the potential to guide LV lead placement in patients with existing pacing systems⁶. Rapid acquisition of 3-dimensional, isotropic, whole heart datasets with sub-millimeter spatial resolution can accurately delineate the coronary venous tree,⁷ non-invasively assess regional and global LV function⁸ and detect regional hypoperfusion/myocardial scar.⁹ Recently CT has evaluated regional and global LV dyssynchrony and areas of LMA by calculating the stretch of the endocardial surface throughout the cardiac cycle (Stretch Quantifier of Endocardial Engraved Zones – SQUEEZ).¹⁰ We hypothesized in patients with existing pacing systems undergoing CRT, pre-procedural cardiac CT-SQUEEZ by targeting areas of late mechanical activation (LMA) and avoiding myocardial scar could guide LV lead placement through identification of the optimal venous target.

Methods

Jump to Section

Go

The study complied with the Declaration of Helsinki and the protocol was approved by the local ethics committee. Informed consent was obtained from each patient. Between September 2014-July 2016 we prospectively recruited 18 patients with a pre-existing pacemaker/ICD, persistent heart failure symptoms on optimal medical therapy, LV ejection fraction (LVEF) $<45\%$ and $>50\%$ right ventricular (RV) pacing.

Pre assessment

Jump to Section

Go

Patients underwent clinical assessment (NYHA score and Minnesota Living with Heart Failure questionnaire), 6-minute walk, cardiopulmonary exercise test and 2-dimensional transthoracic echocardiography. Ischemic etiology (ICM) was defined by prior myocardial infarction, coronary angiography demonstrating severe coronary disease and subsequent revascularization and / or CMR evidence of myocardial fibrosis. Absence of these features inferred non-ischemic cardiomyopathy (NICM).

Cardiac CT

Jump to Section

Go

Patients underwent cardiac CT using a Philips Brilliance iCT 256 MDCT scanner (Philips Healthcare, Best, The Netherlands) pre-upgrade. Intravenous metoprolol was used to achieve a heart rate of <65 beats/min in sinus rhythm and <100 bpm in atrial fibrillation. 120 mls of intravenous contrast (Omnipaque; GE Healthcare, Princeton, NJ, USA) was injected (5ml/s) via power-injector into the antecubital vein. Descending aorta contrast-triggered (180 Hounsfield Units), ECG-gated scanning was performed with single breath hold following a 10-12 second delay. Scanning parameters included a heart rate dependent pitch (0.2-0.45), gantry rotation time of 270 milliseconds, tube voltage of 100 or 120 kVp, depending on the patient's body mass index and a tube current of

ADVERTISEMENT



**PERSONALIZED
CRT**

Claria MRI™
Quad CRT-D

[Watch our Video
to Learn More](#)

Medtronic

125-300 mAs depending on thoracic circumference. A second single phase, ECG-gated scan was acquired 12 minutes after initial contrast bolus for myocardial scar imaging; the kVp was reduced by 20 whilst the mAs was increased proportionately to account for an increase in image noise¹¹. Initial retrospective ECG-gated scans were reconstructed in 10% phase increments throughout the cardiac cycle using iterative reconstruction, with 1mm slice thickness, 0.5mm slice increment, 250 mm field of view, 512x512 matrix and an *Xres smooth* reconstruction kernel. Iterative reconstruction using iDose4 (range 1-7) was used to reduce image noise and reduce the radiation dose. The cardiac CT scan was evaluated by an independent SCCT Level III cardiac CT expert (RR). First pass contrast enhanced sequences were analyzed using standardized multi-planar reconstruction windows according to the AHA nomenclature for regional segmentation. End diastolic myocardial wall thickness was evaluated reviewing each myocardial region in both short and long axis views. Areas of hypoperfusion were evaluated systematically with slice width thickness increased to 5mm, display window and level settings adjusted to 100 and 200 HU respectively. Abnormal perfusion was defined as myocardium exhibiting significantly reduced contrast distribution visually compared against attenuation of normal myocardium in each patient used as an internal reference. Where discrepancies existed a 50 HU difference between normal and hypoperfused myocardium was used^{12, 13} along with consensus opinion from 2 individual experts in cardiac CT (AHA/ACC Level III experience, blinded to the clinical data).

We adopted a pragmatic approach for identifying regions of delayed enhancement as previously described¹¹. This qualitative identification of scar where the myocardium is brighter, reflects the current lack of standard criteria in the literature mainly because the Hu attenuation varies significantly between patients with no accepted value set as a cut-off for fibrosis. Where scar detection was difficult, surrogate markers of a wall thickness <6mm and regional hypoperfusion were used to infer scar.

CT derived Stretch Quantifier of Endocardial Engraved Zones (SQUEEZ) (Figures 1, 2)

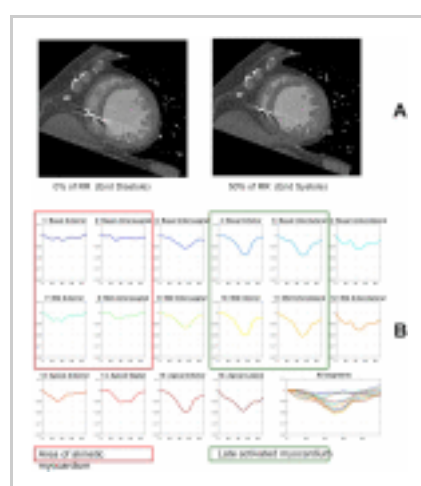


Figure 1

A: CT mid ventricular short axis images of the LV at two time points in the RR interval (0% = end diastole, 50% = end systole). Anterior and antero-septal regions are akinetic and seen not to move throughout the cardiac cycle compared with the infero-lateral segments move inwards by end systole. Inevitable beam hardening artefact from existing pacing system noted in the RV. B: SQUEEZ values (y axis) vs. cardiac cycle length (%) across 16 AHA segments demonstrate akinetic regions (red box) and late activating inferior/infero-lateral walls (green box representing an ideal target for LV lead placement).

[View Large Image](#) | [View Hi-Res Image](#) | [Download PowerPoint Slide](#)

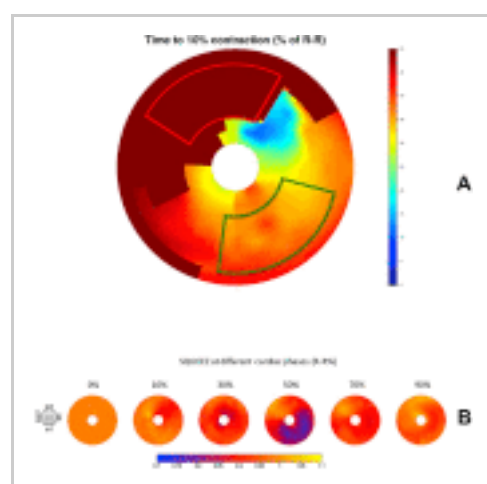


Figure 2

A: Bulls-eye plot of the time delay (color scale, ms) until 10% shortening occurs (ie. time for SQUEEZ to reduce from 1.0 to 0.9) across LV regions. Dark red/brown shows anterior and antero-septal segments not achieving 10% shortening, and likely represents infarcted myocardium. The outlined red box represents areas to avoid (akinetic segments). Red colored regions in the infero-lateral wall show the latest activation away from areas of scar; the outlined green box shows the target pacing regions. B: Bulls-eye plot with color scale representing SQUEEZ values. All segments begin at a SQUEEZ value of 1. Yellow represents >1 (paradoxical stretch/dyskinesis in septal regions). Blue represents SQUEEZ <0.8 and viable regions with reasonable shortening deemed as good targets.

[View Large Image](#) | [View Hi-Res Image](#) | [Download PowerPoint Slide](#)

High contrast disparity between LV blood pool and myocardium permits identification and tracking of finely

engraved endocardial surface features. The SQUEEZ method uses these features to track endocardial material points over the heart cycle to calculate regional cardiac function using the formula:

$$\text{SQUEEZ}(v,t) = \frac{\sqrt{A(v,t)}}{\sqrt{A(v,0)}}$$

Where $A(v,0)$ is the area of the small triangular patch (v) on the endocardial mesh at end diastole and $A(v,t)$ the area of the same patch at time t . The SQUEEZ metric is calculated for each of the triangular patches across the endocardium, through cardiac phases. Thus a high resolution regional map of endocardial strain can be computed as (SQUEEZ-1) at each point. This metric has been correlated to circumferential strain (E_{cc}), the gold standard for non-invasive regional strain, using tagged CMR sequences in a canine model of myocardial infarction¹⁴.

SQUEEZ derived regional function data was merged with individual patient anatomy. Septal segments were excluded as targets. SQUEEZ derived strain curves with low amplitude strain (LAS) <10% shortening were judged non-viable and excluded as targets (analogous to echocardiographic data with poor CRT response with LV lead placement in segments with LAS <9.8%).^{11, 12} Regional time to peak strain (T2P, minimal SQUEEZ value) were calculated using the individual heart rate / cycle length for the CT acquisition. Given the distribution of the coronary veins, the T2P of myocardial segments overlying the same coronary vein were averaged to produce an anterior, lateral and inferior value for mechanical activation delay and compared with hemodynamic data.

CRT implantation

Jump to Section

Go

CRT upgrade was performed with a quadripolar LV lead in 17 (94%) patients and a bipolar lead in 1 due to unfavorable venous anatomy. 9 (50%) patients received a CRTD; 1 patient required an additional RV shock lead, the remaining 8 already having pre-existing ICDs. Identification of the optimal hemodynamic site for LV stimulation was performed by measuring AHR using an 0.014-inch high-fidelity Certus RADI PressureWire (St. Jude Medical, St. Paul, MN, USA) in the LV cavity via a retrograde arterial approach as previously described.¹³ Atrial pacing 10 bpm above intrinsic rate or RV pacing (DDDRV) for patients with no underlying rhythm was baseline. Atrioventricular delays were fixed at 100 milliseconds and ventriculo-ventricular delay 0ms. AHR for each venous site compared biventricular (BV) pacing with baseline (%change, dP/dt_{max} , mmHg/s). AHR was compared with CT indices and the sensed Q-LV at each pacing site.¹⁴ Patients underwent 6 month follow-up to identify clinical responders (CR) via the Packer score¹⁵ and echocardiographic response (ER) defined as reduction in LV end systolic volume (ESV) >15%. The primary endpoint was cardiac CT derived regional endocardial strain analysis (SQUEEZ) prediction of the pacing site achieving the optimal AHR.

Statistics

Jump to Section

Go

Continuous variables were described using mean±standard deviation. Those with Gaussian distribution were compared with a paired t test; if non-Gaussian distribution a Wilcoxon matched-pairs signed rank test. Categorical data was described by absolute number of occurrences and associated frequency (%). Analysis of variance (ANOVA) was used to compare more than two groups. Results were considered significant with a p value <0.05.

Results

Jump to Section

Go

Patient demographics are shown in [table 1](#). Patients had a high percentage of RV pacing with mean QRS duration 173±21ms. 8 (44%) were ischemic.

Table 1

Demographics

	Mean±SD or n(%)
Age (yrs)	68.8 ±15.5
Male	14 (78%)
Ischemic	8 (44%)
RV pacing % pre CRT	92.2 ±17%
LBBB	15 (83%)
QRS duration	173 ±21
Sinus rhythm	16 (89%)
LV End Diastolic Volume (mls)	186 ±65
LV End Systolic Volume (mls)	128 ±62
LV Ejection Fraction (%)	34 ±10

Quality of CT datasets

Jump to Section

Go

All CT scans were successfully completed (mean heart rate 64 ± 7 bpm, mean radiation dose area product (DAP) 1194 ± 419 mGycm².) Patients were supine for 15 ± 1 minutes. Studies were independently assessed using the SCCT quality score¹⁶ (mean score 3.4 ± 1.3 out of 5). The main reason for reduced scoring was beam hardening artefact from existing pacing wires. Wall thinning/hypoperfusion (inferring scar) was present in 7/8 ICM patients however late contrast enhancement was limited to 1 patient.

CT-SQUEEZ derived target segments to predict the optimal venous target

Jump to Section

Go

18 patients underwent successful LV lead implantation and 15/18 had full hemodynamic and CT datasets. In 1 patient a RADI wire was not sited due to arterial access and 2 patients had CT scans of insufficient quality for analysis. CT-SQUEEZ analysis identifying the target epicardial vein subtending the area of LMA excluding LAS regions (inferring scar) was compared with all sites where AHR was measured (3 ± 1 coronary veins/patient). AHR (mean % change) was: $+2.5\pm 8.8\%$ (Anterior), $+14.5\pm 11.5\%$ (Anterolateral), $+23.2\pm 7.7\%$ (Lateral), $+21.8\pm 15.0\%$ (Posterolateral) and $+12.4\pm 5.1\%$ (Posterior), $p=0.001$ (ANOVA). Lateral and posterolateral veins produced the best AHR irrespective of etiology. Lateral vein stimulation produced greater AHR versus the anterior vein (23.2 ± 8.8 vs. $2.5\pm 8.8\%$, $p<0.001$) (Figure 3). Notably 2/15 (13%) patients had no epicardial vein supplying the CT target. In the remaining 13, the CT-SQUEEZ target determined LV implantation site achieving maximal AHR in 9 (70%). A $>10\%$ increase in dP/dt_{max} (positive AHR)¹³ was achieved in 22% anterior, 50% anterolateral, 100% lateral, 80% posterolateral and 67% posterior sites tested. AHR $>10\%$ was achieved in 12/13 (92%) patients with an epicardial vein supplying a CT-SQUEEZ target (the remaining patient had a target AHR of 6.8%).

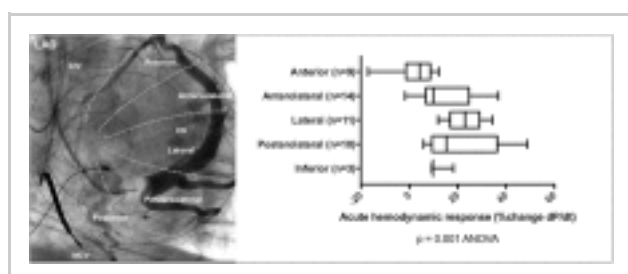


Figure 3

Left: Occlusive venography with nomenclature for coronary venous tree (Reproduced with permission from²⁴). Right: Regional AHR by coronary vein tested. Box and whisker plot for each vein detailing the mean (solid line), range and standard deviation. AHR values are % change in dP/dt versus baseline. There was a significant difference between groups, ANOVA $p=0.001$.

[View Large Image](#) | [View Hi-Res Image](#) | [Download PowerPoint Slide](#)

CT versus hemodynamic/electrical guidance (figure 4)

Jump to Section

Go

CT-SQUEEZ targets produced similar AHR compared with the best achievable AHR ($20.4\pm 13.7\%$ vs $24.9\pm 11.1\%$, $p=0.36$). Targeting electrical latency (longest Q-LV) achieved a similar AHR ($19.4\pm 11.5\%$, $p=0.85$). Pacing scar produced the lowest AHR ($6.8\pm 3.2\%$, $p=0.04$ vs CT) comparable to the worst AHR achievable ($6.4\pm 3.1\%$, $p=0.01$ vs CT). AHR and Q-LV weakly correlated in 63 paired datasets (Pearson $r=0.31$, $p=0.01$). AHR of locations with QLV >100 ms but in scar was significantly lower than non-scarred locations (5.2 ± 1.5 vs. $19.5\pm 9.4\%$, $p=0.005$) (Figure 5).

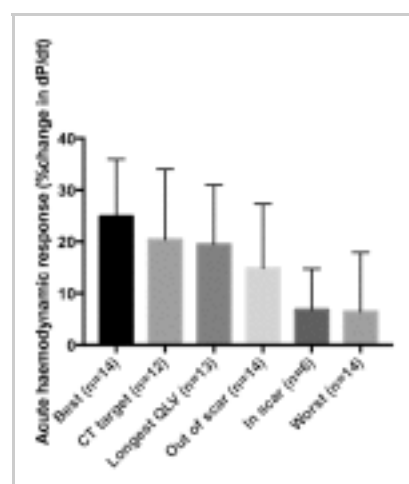


Figure 4

Percentage change AHR determined by pacing the vein with; optimal AHR per patient (Best, $n=14$), the CT-SQUEEZ derived target (CT target, $n=12$), greatest electrical latency (Longest QLV, $n=13$), absence of scar (Out of scar, $n=14$), presence of scar (Scar, $n=6$), the vein with the worst AHR per patient (Worst, $n=14$). Best vs. CT target $p=0.36$, Best vs. Longest QLV $p=0.22$, Best vs. Out of scar $p=0.03$, Best vs. In scar $p=0.002$, Best vs. Worst $p=0.0002$, CT target vs. Longest QLV $p=0.85$, CT target vs. Out of scar $p=0.29$, CT target vs. In scar $p=0.04$, CT target vs. Worst $p=0.009$.

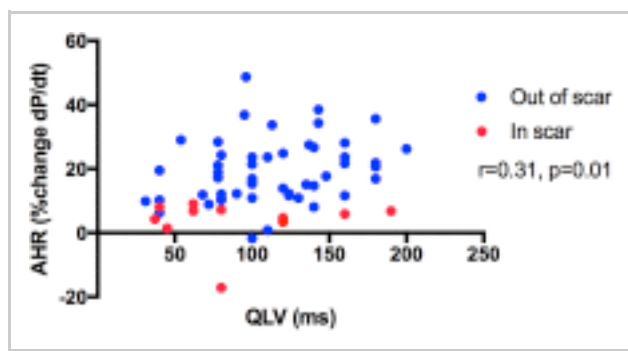


Figure 5

Scatter plot of AHR vs QLV. Each patient had multiple data points acquired. There is a weak correlation between AHR and QLV ($r=0.31$, $p=0.01$). Locations in scar (red) had a lower AHR compared with locations out of scar (blue).

CRT response ([Table 2](#))

Jump to Section

At 6 months patients symptomatically improved (NYHA 1.7 ± 0.7 vs 2.8 ± 0.4 , $p < 0.001$ and MLHF scores 32 ± 24 vs 39 ± 19 , $p = 0.03$) and were able to walk on average 92 meters further over 6 minutes. Paced QRS duration was shorter (142 ± 18 vs 173 ± 21 ms, $p < 0.001$) LVEF increased (34 ± 10 to $44 \pm 15\%$, $p = 0.001$) and NT-pro-BNP reduced (472 ± 459 vs 1121 ± 749 , $p = 0.003$). Patients paced in CT-SQUEEZ targets had greater clinical response compared with non-target segments (90 vs 60%, $p < 0.001$ [Figure 6](#)). 100% of NICM patients were clinical and echocardiographic responders versus only 63% ICM patients ($p = 0.07$).

Table 2

CRT response.

	Pre assessment	6m follow up	P value
NYHA class symptoms	2.8 ± 0.4	1.7 ± 0.7	< 0.001
MLHF questionnaire points	39 ± 19	32 ± 24	0.03
6 minute walking distance	291 ± 137	383 ± 154	0.06
Paced QRS duration (ms)	173 ± 21	142 ± 18	< 0.001
CPET, VO2 max (mls/min/kg)	17.9 ± 4	18.1 ± 5	0.84
CPET, Slope @ VO2 max	36 ± 9	34 ± 5	0.88
LV End Diastolic Volume (mls)	186 ± 65	154 ± 61	0.01
LV End Systolic Volume (mls)	128 ± 62	93 ± 60	0.01
2D LVEF (TTE)	34 ± 10	44 ± 15	0.001
NT-pro-BNP	1121 ± 749	472 ± 459	0.003

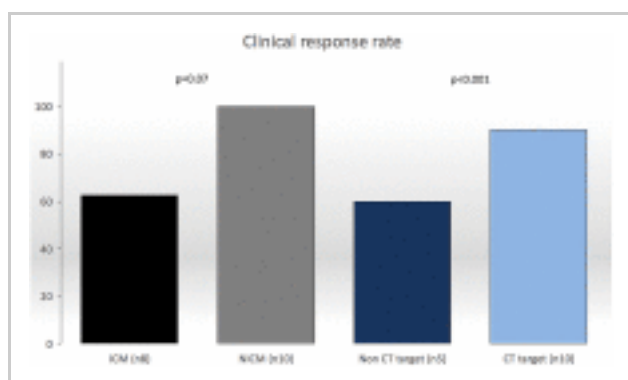


Figure 6

Clinical response rates in CT-SQUEEZ target ($n=10$) versus non target ($n=5$), ($p < 0.001$) and ICM ($n=8$) versus NICM ($n=10$), ($p = 0.07$).

Discussion

Jump to Section

The principal findings were:

Jump to Section

- 1) CT-SQUEEZ targets produced similar mean AHR compared with the best achievable AHR ($20.4 \pm 13.7\%$ vs $24.9 \pm 11.1\%$, $p = 0.36$).
- 2) CT-SQUEEZ guidance produced positive AHR in 92% of cases when a target segment was paced.

3) Pacing a CT-SQUEEZ target vein produced greater clinical response versus non-target segments (90 vs 60%).

We demonstrate the novel utility of pre-procedural CT for LV lead guidance to regions of LMA devoid of LAS. [Figures 1](#) and [2](#) show cardiac CT sequences were able to generate functional datasets with sufficient temporal resolution to differentiate the region of LMA. In addition to wall thinning and hypo-perfusion the SQUEEZ algorithm inferred regions of scar on the basis of LAS in keeping with echocardiographic studies (defined LAS as radial strain <10%) resulting in sub-optimal response to CRT.¹⁵ Our CT protocol included a late enhancement sequence to identify fibrosis, however we only identified late enhancement in 1 patient. Our CT-SQUEEZ derived algorithm predicted regions with an AHR within 2.5% of the maximum in 11/12 cases (92%). Additionally, patients paced in CT targets had a more favorable response ([Figure 4](#)). In one case, the mismatch between the CT target and the vein with the best AHR was significant (22.2%). In 2 cases, CT-SQUEEZ targeted the posterior wall however the patients had no epicardial vein overlying this site.

The clinical utility of AHR >10% in predicting CRT response has been demonstrated¹⁶ and using this cut off, a high proportion of CT targets had positive AHR. There was a trend towards greater AHR in sites out of scar versus CT inferred scar (14.8±12 vs. 6.8±8%, p=0.17). Mean AHR was similar in CT targets compared with Q-LV ([Figure 4](#)) reflecting a correlation between electrical and mechanical dyssynchrony. However, regions with electrical latency (QLV>100ms) in scar resulted in sub-optimal AHR suggesting Q-LV alone may fail to identify the optimal stimulation site in the presence of scar.

We previously demonstrated CMR derived scar and dyssynchrony can guide LV lead implantation¹⁷ with excellent CRT response if pacing in a CMR target in keeping with the current findings. Similarly, Laksman et. al used CMR derived scar and dyssynchrony guided lead placement with echocardiographic super-response in 58% patients.¹⁸ Currently there is limited clinical data describing the use of cardiac CT LV lead guidance.¹⁹ Two randomized controlled studies TARGET²⁰ and STARTER²¹ have shown benefit with LV lead guidance using speckle tracking echocardiography.

Scar avoidance using CMR derived late gadolinium enhancement is associated with improved cardiovascular outcomes.²² The ability of CMR to accurately define scar is superior to CT, however almost a third of patients undergoing CRT have existing pacemakers unsuitable for CMR.⁵ Cardiac CT offers several potential advantages over CMR. Images of superior spatial resolution within a 3D isotropic dataset are acquired within a matter of seconds; the new generation of CT scanners producing images in a single heartbeat. Additionally, exquisite differentiation of endocardium and blood pool enables accurate tracking of regional surfaces over the duration of the cardiac cycle. Delayed triggered contrast enhanced sequences facilitate good opacification of the coronary venous tree and volume rendered reconstructions can delineate the course of potential venous targets pre-implantation. This may be particularly advantageous as coronary venous anatomy is highly variable and may impact successful CRT delivery²³. Furthermore, identification of CS valves and highly angulated/tortuous vessels may help in patients with a previously failed implant. Whilst targeting regions of LMA is scientifically sound, LV lead placement is restricted by coronary vein anatomy which may not always overly the optimal region. In a cardiac CT study of 121 post mortem hearts, 29% had no coronary vein overlaying the postero-lateral region.²⁴ Lack of a venous target identified by pre-procedural CT may allow alternative forms of LV stimulation (multi-site/endocardial) to be considered.^{25, 26}

Limitations

Jump to Section



Go

Modern single source / energy CT scanners are currently unable to accurately delineate extracellular myocardial fibrosis through late contrast enhancement. Whilst iodinated contrast displays similar kinetic properties to gadolinium-DTPA, and can demonstrate acute hypoperfusion from ischemic injury, reliable visualization of chronic fibrosis with late enhancement occurred in only 1 patient. We therefore used local wall thinning (<6mm) and / or hypoperfusion to infer scar and the low AHR in these segments is in keeping with scar despite the lack of visualization ([Figure 4](#), [Figure 5](#)). The presence of existing pacing systems resulting in beam hardening artefact and degradation of signal in myocardial tissue local to the pacing leads may explain this. One study reporting a good correlation between late enhancement and scar at histological macroscopy in a chronic porcine model²⁵ used higher contrast doses than our study (145±35ml vs. 120±0mls, p=0.005) and the animals had no pre-existing pacing systems. The development of dual energy / source CT scanners holds promise in improving differentiation between subtle soft tissue characteristics and may be able to more reliably demonstrate myocardial fibrosis.²⁷ The temporal resolution of cardiac CT in this study (70-100ms) is inferior to echocardiography (20ms) and CMR (35-50ms, obtained over multiple beats) and cardiac CT may be less sensitive to subtle regional motion changes. Whilst SQUEEZ detects motion abnormalities with high resolution, only lower resolution estimates (16 standard AHA segments) were needed. Furthermore, the CT-SQUEEZ derived metric has been shown to correlate well with circumferential strain (E_{cc}) in an animal model suggesting it is sensitive enough to demonstrate local regional motion differences and remain a useful tool to assess for dyssynchrony¹⁴. The utility of AHR in predicting CRT response¹⁶ is limited and the results of a large, multi-center randomized trial of AHR are awaited (RADI-CRT, NCT01464502).

Conclusions

Jump to Section



Go

Pre procedural CT-SQUEEZ derived target selection may be a valuable tool to predict the optimal venous site for

Acknowledgement of support.

Jump to Section

Go

JMB and SC acknowledge support of the NIHR BRC at Guy's and St Thomas' NHS Foundation Trust. JMB acknowledges the support of the Rosetrees trust. The authors acknowledge the support of the Department of Radiology, Guy's and St Thomas' Hospital led by Paul Woodburn and Dan Hodson and support of the Healthcare Technology Cooperative.

Appendix A. Supplementary data

Jump to Section

Go

[View File](#)

References

Jump to Section

Go

1. Curtis, A.B., Worley, S.J., Adamson, P.B., Chung, E.S., Niazi, I., Sherfese, L., Shinn, T., and Sutton, M.S.J. **Biventricular pacing for atrioventricular block and systolic dysfunction.** *N Engl J Med.* 2013; 368: 1585–1593

[View in Article](#) | [Crossref](#) | [PubMed](#) | [Scopus \(198\)](#)

2. Bleeker, G.B. **Kaandorp T a M, Lamb HJ, Boersma E, Steendijk P, de Roos A, Van Der Wall EE, Schalij MJ, Bax JJ: Effect of posterolateral scar tissue on clinical and echocardiographic improvement after cardiac resynchronization therapy.** *Circulation.* 2006; 113: 969–976

[View in Article](#) | [Crossref](#) | [PubMed](#) | [Scopus \(555\)](#)

3. Ypenburg, C., van Bommel, R.J., and Delgado, V. **Mollema S a, Bleeker GB, Boersma E, Schalij MJ, Bax JJ: Optimal left ventricular lead position predicts reverse remodeling and survival after cardiac resynchronization therapy.** *J Am Coll Cardiol.* 2008; 52: 1402–1409

[View in Article](#) | [PubMed](#) | [Scopus \(272\)](#)

4. Leyva, F. **Cardiac resynchronization therapy guided by cardiovascular magnetic resonance.** *J Cardiovasc Magn Reson.* 2010; 12: 64

[View in Article](#) | [Crossref](#) | [PubMed](#) | [Scopus \(21\)](#)

5. Daubert, J.-C., Saxon, L., Adamson, P.B. et al. **2012 EHRA/HRS expert consensus statement on cardiac resynchronization therapy in heart failure: implant and follow-up recommendations and management.** *Europace.* 2012; 14: 1236–1286

[View in Article](#) | [Crossref](#) | [PubMed](#)

6. Mak, G.S., Truong, Q.A., and Cardiac, C.T. **Imaging of and Through Cardiac Devices.** *Curr Cardiovasc Imaging Rep.* 2012; 5: 328–336

[View in Article](#) | [Crossref](#) | [PubMed](#) | [Scopus \(10\)](#)

7. Sun, C., Pan, Y., Wang, H., Li, J., Nie, P., Wang, X., Ma, H., and Huo, F. **Assessment of the coronary venous system using 256-slice computed tomography.** *PLoS One.* 2014; 9: e104246

[View in Article](#) | [Crossref](#) | [PubMed](#) | [Scopus \(4\)](#)

8. Truong, Q a, Singh, J.P., Cannon, C.P. et al. **Quantitative analysis of intraventricular dyssynchrony using wall thickness by multidetector computed tomography.** *JACC Cardiovasc Imaging American College of Cardiology Foundation.* 2008; 1: 772–781

[View in Article](#) | [Crossref](#) | [Scopus \(39\)](#)

9. Truong, Q.A., ee, Thai W., Wai, B. et al. **Myocardial scar imaging by standard single-energy and dual-energy late enhancement CT: Comparison with pathology and electroanatomic map in an experimental chronic infarct porcine model.** *J Cardiovasc Comput Tomogr.* 2014; 9: 313–320

[View in Article](#) | [Abstract](#) | [Full Text](#) | [Full Text PDF](#) | [Scopus \(4\)](#)

10. Pourmorteza, A. and Schuleri, K.H. **Herzka D a, Lardo AC, McVeigh ER: A new method for cardiac computed tomography regional function assessment: stretch quantifier for endocardial engraved zones (SQUEEZ).** *Circ Cardiovasc Imaging.* 2012; 5: 243–250

[View in Article](#) | [Crossref](#) | [PubMed](#) | [Scopus \(18\)](#)

11. Mendoza, D.D., Joshi, S.B., Weissman, G., Taylor, A.J., and Weigold, W.G. **Viability imaging by cardiac computed tomography.** *J Cardiovasc Comput Tomogr.* 2010; 4: 83–91

[View in Article](#) | [Abstract](#) | [Full Text](#) | [Full Text PDF](#) | [PubMed](#) | [Scopus \(19\)](#)

12. Nieman, K., Cury, R.C., Ferencik, M., Nomura, C.H., Abbara, S., Hoffmann, U., Gold, H.K., Jang, I.-K., and Brady, T.J. **Differentiation of recent and chronic myocardial infarction by cardiac computed tomography.** *Am J Cardiol.* 2006; 98: 303–308

[View in Article](#) | [Abstract](#) | [Full Text](#) | [Full Text PDF](#) | [PubMed](#) | [Scopus \(74\)](#)

13. Blankstein, R., Rogers, I.S., and Cury, R.C. **Practical tips and tricks in cardiovascular computed tomography: Diagnosis of myocardial infarction.** *J Cardiovasc Comput Tomogr.* 2009; 3: 104–111

[View in Article](#) | [Abstract](#) | [Full Text](#) | [Full Text PDF](#) | [PubMed](#) | [Scopus \(22\)](#)

14. Pourmorteza, A., Chen, M.Y., Pals, J., Arai, A.E., and Mcveigh, E.R. **Correlation of CT-based regional**

cardiac function (SQUEEZ) with myocardial strain calculated from tagged MRI: an experimental study. *Int J Cardiovasc Imaging.* 2016; 32: 817–823

[View in Article](#) | [Crossref](#) | [PubMed](#) | [Scopus \(1\)](#)

15. Khan, F.Z., Virdee, M.S., Read, P.A. et al. **Effect of Low-Amplitude Two-Dimensional Radial Strain at Left Ventricular Pacing Sites on Response to Cardiac Resynchronization Therapy.** *J Am Soc Echocardiogr.* 2010; 23: 1168–1176

[View in Article](#) | [Abstract](#) | [Full Text](#) | [Full Text PDF](#) | [PubMed](#) | [Scopus \(27\)](#)

16. Duckett, S.G., Ginks, M.R., Shetty, A.K., Bostock, J., Gill, J.S., Hamid, S., Kapetanakis, S., Cunliffe, E., Razavi, R., Carr-White, G., and Rinaldi, C.A. **Invasive acute hemodynamic response to guide left ventricular lead implantation predicts chronic remodeling in patients undergoing cardiac resynchronization therapy.** *J Am Coll Cardiol.* 2011; 58: 1128–1136

[View in Article](#) | [PubMed](#) | [Scopus \(63\)](#)

17. Shetty, A.K., Duckett, S.G., Ginks, M.R. et al. **Cardiac magnetic resonance-derived anatomy, scar, and dyssynchrony fused with fluoroscopy to guide LV lead placement in cardiac resynchronization therapy: a comparison with acute haemodynamic measures and echocardiographic reverse remodelling.** *Eur Heart J Cardiovasc Imaging.* 2013; 14: 692–699

[View in Article](#) | [Crossref](#) | [PubMed](#) | [Scopus \(25\)](#)

18. Laksman, Z., Yee, R., Stirrat, J. et al. **Model-based Navigation of Left and Right Ventricular Leads to Optimal Targets for Cardiac Resynchronization Therapy: A Single Centre Feasibility Study.** *Circ Arrhythm Electrophysiol.* 2014; 7: 1040–1047

[View in Article](#) | [Crossref](#) | [PubMed](#) | [Scopus \(2\)](#)

19. Zhou, W., Hou, X., Piccinelli, M., Tang, X., Tang, L., Cao, K., Garcia, E.V., Zou, J., and Chen, J. **3D Fusion of LV Venous Anatomy on Fluoroscopy Venograms With Epicardial Surface on SPECT Myocardial Perfusion Images for Guiding CRT LV Lead Placement.** *JACC Cardiovasc Imaging.* 2014; 7: 1239–1248

[View in Article](#) | [Crossref](#) | [PubMed](#) | [Scopus \(9\)](#)

20. Khan, F.Z., Virdee, M.S., Palmer, C.R., Pugh, P.J., O'Halloran, D., and Elsik, M. **Read P a, Begley D, Fynn SP, Dutka DP: Targeted left ventricular lead placement to guide cardiac resynchronization therapy: the TARGET study: a randomized, controlled trial.** *J Am Coll Cardiol.* 2012; 59: 1509–1518

[View in Article](#) | [PubMed](#) | [Scopus \(251\)](#)

21. Saba, S., Marek, J., Schwartzman, D., Jain, S., Adelstein, E., and White, P. **Oyenuga O a, Onishi T, Soman P, Gorcsan J: Echocardiography-guided left ventricular lead placement for cardiac resynchronization therapy: results of the Speckle Tracking Assisted Resynchronization Therapy for Electrode Region trial.** *Circ Heart Fail.* 2013; 6: 427–434

[View in Article](#) | [Crossref](#) | [PubMed](#) | [Scopus \(106\)](#)

22. Leyva, F., Foley, P.W.X., Chalil, S., Ratib, K., Smith, R.E., Prinzen, F., and Auricchio, A. **Cardiac resynchronization therapy guided by late gadolinium-enhancement cardiovascular magnetic resonance.** *J Cardiovasc Magn Reson.* 2011; 13: 29

[View in Article](#) | [Crossref](#) | [PubMed](#) | [Scopus \(72\)](#)

23. Singh, J.P., Houser, S., Heist, E.K., and Ruskin, J.N. **The Coronary Venous Anatomy.** *J Am Coll Cardiol.* 2005; 46: 68–74

[View in Article](#) | [PubMed](#) | [Scopus \(123\)](#)

24. Spencer, J.H., Larson, A.A., Drake, R., and laizzo, P.A. **A detailed assessment of the human coronary venous system using contrast computed tomography of perfusion-fixed specimens.** *Heart Rhythm.* 2014; 11: 282–288

[View in Article](#) | [Abstract](#) | [Full Text](#) | [Full Text PDF](#) | [PubMed](#) | [Scopus \(6\)](#)

25. Rinaldi, C.A., Burri, H., Thibault, B., Curnis, A., Rao, A., Gras, D., Sperzel, J., Singh, J.P., Biffi, M., Bordachar, P., and Leclercq, C. **A review of multisite pacing to achieve cardiac resynchronization therapy.** *Europace.* 2015; 17: 7–17

[View in Article](#) | [Crossref](#) | [PubMed](#) | [Scopus \(19\)](#)

26. Behar, J.M., Jackson, T., Hyde, E., Claridge, S., Gill, J., Bostock, J., Sohal, M., Porter, B., O'Neill, M., Razavi, R., Niederer, S., and Rinaldi, C.A. **Optimized Left Ventricular Endocardial Stimulation Is Superior to Optimized Epicardial Stimulation in Ischemic Patients With Poor Response to Cardiac Resynchronization Therapy.** *JACC Clin Electrophysiol.* 2016; 2: 799–809

[View in Article](#) | [Crossref](#) | [PubMed](#) | [Scopus \(1\)](#)

27. Hamilton-Craig, C., Seltmann, M., Ropers, D., and Achenbach, S. **Myocardial viability by dual-energy delayed enhancement computed tomography.** *JACC Cardiovasc Imaging.* 2011; 4: 207–208

[View in Article](#) | [Crossref](#) | [PubMed](#) | [Scopus \(6\)](#)

Disclosures: SC has received research funding from Abbott. TJ and BS have received research funding from Medtronic Inc. CAR receives research funding from Abbott & Medtronic. ERM owns founder's shares in MRI Interventions Inc.

© 2017 Published by Elsevier Inc. on behalf of Heart Rhythm Society.

Advertisements on this site do not constitute a guarantee or endorsement by the journal, Association, or publisher of the quality or value of such product or of the claims made for it by its manufacturer.